This article was downloaded by: *[Matikas, T. E.]*
On: *3 March 2009*
Access details: *Access Details: [subscription number 909207749]*
Publisher *Taylor & Francis*
Informa Ltd Registered in England and Wales Registered Number: 1072954 Registered office: Mortimer House, 37-41 Mortimer Street, London W1T 3JH, UK

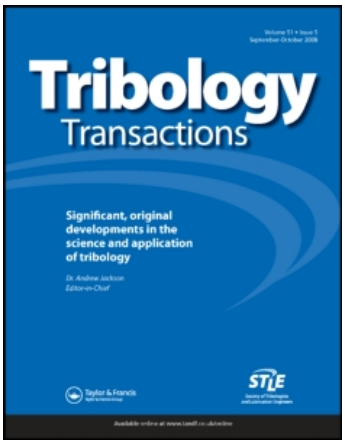

Tribology Transactions
Publication details, including instructions for authors and subscription information:
http://www.informaworld.com/smpp/title~content=t713669620

Prediction of Contact Temperature Distribution during Fretting Fatigue in Titanium Alloys

T. E. Matikas [a]; P. D. Nicolaou [a]
[a] Mechanical Behavior and Quality Control Laboratory, Department of Materials Science and Engineering, University of Ioannina, University Campus, Ioannina, Greece

First Published on: 01 May 2009

To cite this Article Matikas, T. E. and Nicolaou, P. D.(2009)'Prediction of Contact Temperature Distribution during Fretting Fatigue in Titanium Alloys',Tribology Transactions,52:3,346 — 353
To link to this Article: DOI: 10.1080/10402000802563117
URL: http://dx.doi.org/10.1080/10402000802563117

PLEASE SCROLL DOWN FOR ARTICLE

Full terms and conditions of use: http://www.informaworld.com/terms-and-conditions-of-access.pdf

This article may be used for research, teaching and private study purposes. Any substantial or systematic reproduction, re-distribution, re-selling, loan or sub-licensing, systematic supply or distribution in any form to anyone is expressly forbidden.

The publisher does not give any warranty express or implied or make any representation that the contents will be complete or accurate or up to date. The accuracy of any instructions, formulae and drug doses should be independently verified with primary sources. The publisher shall not be liable for any loss, actions, claims, proceedings, demand or costs or damages whatsoever or howsoever caused arising directly or indirectly in connection with or arising out of the use of this material.

Tribology Transactions, 52: 346-353, 2009
Copyright © Society of Tribologists and Lubrication Engineers
ISSN: 1040-2004 print / 1547-397X online
DOI: 10.1080/10402000802563117

Downloaded By: [Matikas, T. E.] At: 22:02 3 March 2009

Prediction of Contact Temperature Distribution during Fretting Fatigue in Titanium Alloys

T. E. MATIKAS and P. D. NICOLAOU
Mechanical Behavior and Quality Control Laboratory
Department of Materials Science and Engineering
University of Ioannina, University Campus
45110 Ioannina, Greece

Fretting is a critical problem to the manufacturers and operators of turbine engines, reducing the useful life of fan, compressor, and turbine blade components. The fretting action between the two components in contact leads to temperature rise, which in most cases, may be significant enough to cause a number of adverse effects. The knowledge of the temperature profiles inside the material is very important because it enables the prediction of possible oxide formation and the development of thermal stresses. To this end, the temperature profile for Ti-6Al-4V alloys has been predicted in this work utilizing a heat flow channel (HFC) model. The model requires as input the material constants (thermal conductivity, thermal diffusivity, and flow stress), the material surface characteristics (roughness and asperity spacing), the frictional conditions between the two surfaces, as well as the external parameters (frequency, amplitude of oscillation, magnitude of contact area). The analysis enabled the determination of the temperature field as a function of time and the three spatial coordinates. The model showed that the temperature increases quite rapidly at the beginning of the process and reaches an essentially constant value after approximately 1000 cycles. The predictions revealed a rapid decay of temperature with the thickness of the specimen, while the temperature drop was found to be much smoother in the other two specimen directions. Additionally, a first-order validation of the model was achieved by determining the oxygen concentration in fretting-fatigued Ti-6Al-4V specimens, where it was found that an increased oxygen concentration existed in the fretting area compared to the non-contact and stick areas.

KEY WORDS

Fretting Fatigue; Titanium Alloys; Ti-6Al-4V; EDS; Heat Conduction

Manuscript received January 28, 2008
Manuscript accepted October 14, 2008
Review led by Bob Bruce

INTRODUCTION

Titanium-based alloys are widely used in the aerospace industry due to their high strength/weight ratio and good corrosion resistance. The applications for titanium alloys as aircraft engine structural components include fan, low-pressure compressor disks, and blades. Aircraft turbine engines are high rotating speed, flexible machines that operate over wide ranges of temperatures, pressures, speeds, and external as well internal stresses, and, as all types of rotating machines are susceptible to fretting. One potential catastrophic result of fretting damage is the adverse effect on the fatigue life of mechanical components. In such situations fretting is critical to the reliable operation through the entire service life of the engine and frequently contributes to critical failures.

Fretting corrosion and fretting fatigue occur when the oscillatory tangential relative movement of two tight-fitting surfaces is combined with an applied axial load. Fretting is a wear phenomenon, adhesive in nature, and vibration is its essential contributing factor. Fretted areas are highly sensitive to fatigue cracking. Under fretting conditions fatigue cracks can nucleate at relatively low loads. Nucleation of fatigue cracks in fretted regions depends mainly on the state of stress on the surface and particularly on the stresses superimposed on the cyclic stress. Secure clamping to prevent relative slip between the surface elements is recognized as one approach to prevent fretting; however, it is not a feasible approach in a lightweight flexible machine such as an aircraft turbine engine. Although the detrimental impact of fretting on fatigue life of titanium alloys has been studied, an overall understanding of the nature of the fretting fatigue process is far from complete (Hoeppner and Goss *(1)*; Wharton and Waterhouse *(2)*; Lutynski, et al. *(3)*; Nicolaou, et al. *(4)*; Nakazawa, et al. *(5)*; Antoniou and Radtke *(6)*; Asai *(7)*; Lee, et al. *(8)*; Golden, et al. *(9)*; Matikas and Nicolaou *(10))*.

It is generally accepted that one of the most important parameters in all sliding contact systems is the temperature field in the vicinity of the sliding surfaces. The temperature field around the contact asperity significantly affects the material properties, its micro-structure, and the oxidation process. Early work, based on the observation that a low melting polymer produced fretting on steel without exhibiting signs of melting, led to the conclusion that there was little if any temperature rise in fretting (Wright *(11)*).

Downloaded By: [Matikas, T. E.] At: 22:02 3 March 2009

However, observations on X-ray diffraction patterns obtained in fretting fatigue experiments on bright drawn mild steel (Waterhouse *(12)*) indicated that there were temperature effects. The pattern obtained from the unfretted surface showed no resolution of the Kα doublet in the highest angle line (310 reflection using Co Kα radiation) due to the cold-worked nature of the material. In the fretted region the doublet was resolved, showing that some annealing action had occurred. From the degree of resolution the temperature rise in the fretted region was estimated at 500°C. The surface was then progressively etched away with acid until the original unresolved doublet of the material was obtained. The depth of the heat-affected zone was estimated at about 125 μm. Later work, where a bead of a thermocouple was fretted against a steel surface, confirmed these observations (Alyabev, et al. *(13)*). Temperature rises of 300°C to 500°C were observed with thermal spikes reaching as high as 800°C. The type of alloy that is likely to be most sensitive to the lower general temperature rise is the age-hardened alloy, which again includes $\alpha + \beta$ titanium alloys and many of the aluminum alloys. Temperature rises into the 800°C to 1000°C region, however, would greatly influence the $\alpha + \beta$ titanium alloys since the β transus would be crossed.

There has been very little experimental work in this field. It should be pointed out that most measurements of this temperature rise have been made on steel. Fretting fatigue studies in steel revealed microstructural transformation during the process. One of the mechanisms that could possibly cause microstructural transformation in these materials during fretting fatigue has been related to the significant increase in local temperature (Archard and Rowntree *(14)*; Vodopivec, et al. *(15)*; Podgornik, et al. *(16)*; Kalin and Vizintin *(17)*, *(18)*). The region experiencing such local temperature increases was subsequently quenched by the surrounding material, leading to a fine-grained martensitic structure. Similar behavior has been reported after fretting fatigue experiments on PH 13-8 Mo stainless steel using flat fretting pads (Pape and Neu *(19)*). In this case, a number of transformed regions were observed, which were likely due to a significant refinement in grain size. It is believed that this region is formed due to the high shear stresses and strains at the contact, but that local increase in temperature assists the process (Pape and Neu *(20)*).

The temperature rise due to fretting fatigue can influence the process in a variety of ways, notably by controlling the oxidation rate at the interface, the absorption of gases and lubricants, the mechanical properties of the surface layers, and the viscosity of the lubricant (Sarkar *(21)*; Barber *(22)*). The energy dissipated in sliding is almost entirely converted into heat at or near the contact surface. Owing to the inevitable roughness of the surfaces, the contact at any particular time is restricted to a few small areas, which are distributed over the nominal contact areas. Therefore, high temperatures are reached at these actual contact areas. Early experimental work has established values for these thermal spikes, which approach the melting point of the solids. However, although very high temperatures are reached at the surface, the small quantity of heat liberated at each actual contact area makes it impossible for the effect to penetrate far into the solid. Irregularities in the temperature field due to non-uniform heat input will only be detectable to a depth that is comparable with the linear dimensions of the actual area of contact. Thus, flash temperatures due to thermal spikes are very difficult to measure (Dow *(23)*; Beck *(24)*). For this reason a few experimental data are available in the literature. The graph in Fig. 1 shows data of Alyabev, et al. *(13)* that measured temperatures above 400°C near the fretting pad during fretting fatigue experiments in steel.

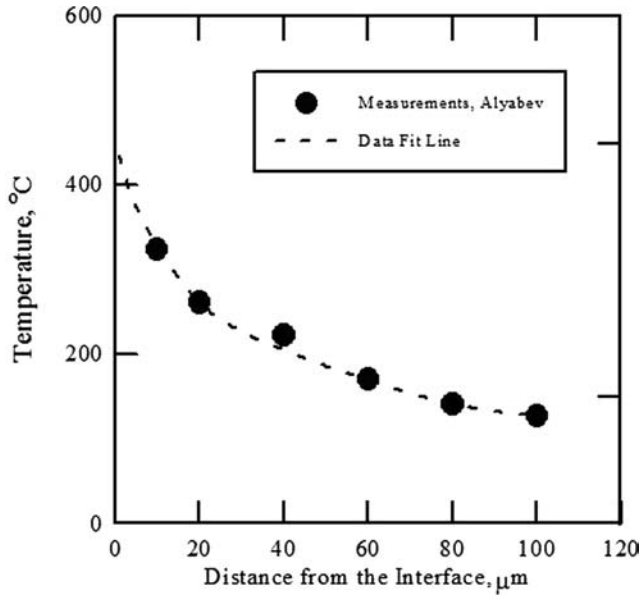

Fig. 1—Experimental data of Alyabev, et al. *(13)*, of temperature vs. the distance from the fretting pad during fretting fatigue experiments, showing that the temperature exceeds 400°C at the origin.

The knowledge of the temperature profile inside the materials is very important because it enables the prediction of possible oxide formation, interface thermal softening, development of thermal stresses, and possible local material melting. Therefore, this work aims to predict the temperature profile as a function of time and the spatial coordinates using a heat flow channel model. The model predictions that are presented in this article correspond to the temperature profile of a Ti-6Al-4V alloy undergoing fretting fatigue. In addition, in order to examine the validity of the magnitude of the temperature rise predicted by the model, the oxygen concentration in a fretting-fatigued specimen has been determined.

HEAT TRANSFER MODEL

The essential features of sliding systems that influence heat flow are the nature of the contact between the solids, the distribution of the heat sources, and the large-scale cooling effects at the non-contacting surfaces.

Boundary Conditions

Area of Contact

The area at each surface within which contact is possible will be defined by the geometry of the sliding system; this is known as the nominal contact area. However, the roughness of surfaces restricts the actual contact to a number of small areas at the peaks of the surface asperities. As the normal load is increased, these asperities deform, allowing the solids to move closer together and causing more contact areas to be formed. Thus, the contact of

sliding solids is restricted to a number of small areas. However, in this case the distortion produced by the relative motion of the solids will cause the actual contact areas either to be transient due to the fracture of the junctions or more relative to one or both solids (Mimic *(25)*).

Location of Heat Sources

The heat generated during sliding influences the adhesion, deformation, and the fracture behaviors of the contacting materials in relative motion. Temperature interacts with the fretting process in two ways: first, the rate of oxidation or corrosion increases with temperature, and second, the mechanical properties, such as the hardness of the materials are also temperature dependent (Bill *(26)*). Earlier experimental work on large-scale model junctions further supports the general proposition that most of the heat is generated within the sphere of which the actual contact area forms a diametrical plane (Dow *(23)*).

Large-Scale Cooling Effects

It can be argued that if the distance between the cooled boundaries of the solids and the interface is large in comparison with the dimensions of the actual contact (as it is generally the case), it is possible to approximate the system to two semi-infinite solids. It is true that the temperatures at such remote regions of the semi-infinite solids are scarcely affected by the conditions at the interface. However, the material beyond these imaginary boundaries performs the function of a tan infinite heat sink of negligible thermal resistance. In a finite system in a steady thermal state, of an infinite heat sink is replaced by a practical heat-transfer process that causes the average temperature of the boundaries to be related to the heat flow from them.

In the contact of two semi-infinite solids, the temperature at infinity is unaffected by any changes in the temperature at the contact area (assumed finite), but the temperature at infinity does affect the temperature field near the contact area. Similarly, even if the boundaries of the two finite solids are sufficiently remote from the interface to be unaffected by contact conditions there, the temperature field near the contact area and the distribution of heat between the solids will be affected by the temperature of the boundaries. In fact, this practical system can be approximated to two semi-infinite solids with the same contact conditions but of which the temperatures at infinity are related to the heat flow rates by the following equations:

$$Q_1 = f(T_1), \quad Q_2 = f(T_2) \qquad [1]$$

where Q_1, Q_2 are the rates of heat flow through the solids 1 and 2, respectively, and T_1, T_2 are the temperatures of their exposed surfaces (Barber *(22)*; Wang and Komvopoulos *(27)*; Yeo and Barber *(28)*; Attia and D'Silva *(29)*).

TEMPERATURE PROFILE

If the contact conditions and the heat sources distributions are specified, the problem is essentially similar to that of a single contact area with a non-uniform distribution of heat sources. A numerical solution could be obtained from a series of linear simultaneous equations by a suitable subdivision of the discontinuous contact area. An idealized contact configuration within a single contour area viewing the array of micro-contact areas is shown in Fig. 2. The model is based on the following assumptions/considerations:

(i) The contact between the two rough surfaces is equivalent to the contact between a perfectly flat rigid plane and an equivalent rough surface.
(ii) The contact pressure and shear traction are assumed to be uniformly distributed over the micro-contact area. The flow stress of the softer material and the coefficient of friction of are assumed to be constant.

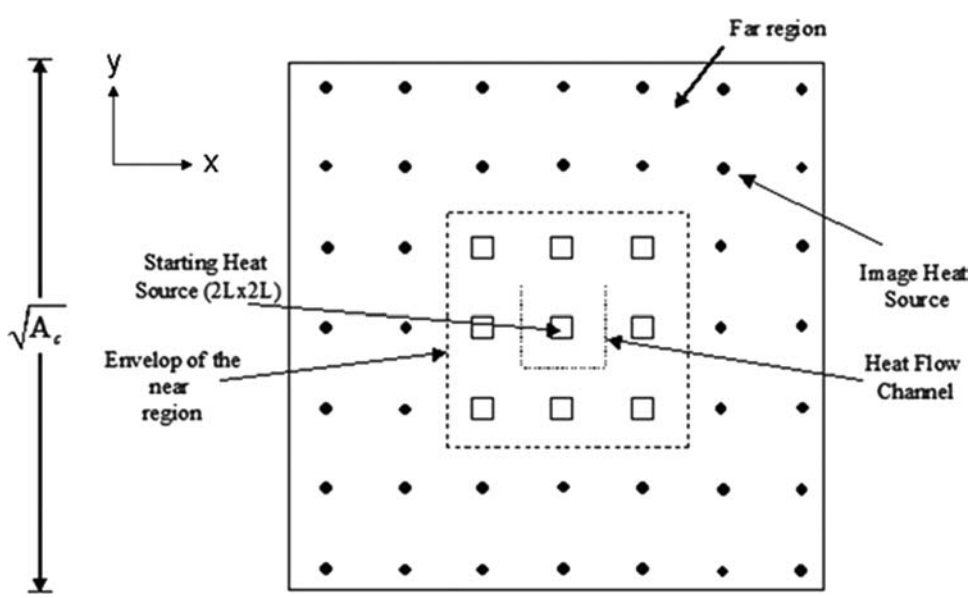

Fig. 2—Idealized contact configuration within a single contour area A_c; view of the array of micro-contact areas (frictional heat source).

Downloaded By: [Matikas, T. E.] At: 22:02 3 March 2009

Downloaded By: [Matikas, T. E.] At: 22:02 3 March 2009

(iii) The micro-contacts are squares (sides 2L) and are uniformly distributed over the contour area as shown in Fig. 2.
(iv) Except for the micro-contact areas, the asperities and the control surface of the heat flow channel are adiabatic.
(v) The semi-infinite body oscillates in a simple harmonic motion.
(vi) The thermal and mechanical properties of the material are temperature independent.
(vii) The contact configuration does not change with the temperature rise.

Assuming sliding and static contact, the temperature rise $\theta(x, y, z, t)$ at any point within the heat flow channel is a linear superposition of the contribution of its own frictional heat source θ_{shs} (labeled as the starting heat source in Fig. 2) and that of the neighboring image sources θ_{ihs}. The contribution of the image sources is grouped into two regions to simplify the analysis: the near and far regions θ_{nr} and θ_{fr}, respectively.

Thus,

$$\theta(x, y, z, t) = [\theta_{shs}] + \sum_{j=1}^{N_t-1} [\theta_{ihs}]_j = [\theta_{shs}] + \sum_{j=1}^{N_{nr}-1} [\theta_{ihs}]_j + [\theta_{fr}] \quad [2]$$

where N_t and N_{nr} are the total number of micro-contacts within the contour area and the near region, respectively. Each of the terms given in the above Eq. [2], namely θ_{shs}, θ_{nr}, and θ_{fr}, can be obtained from the fundamental solution for the temperature rise $\theta(x, y, z, t)$ at point $P(x, y, z)$ and time t due to a single square heat source $(2\delta' \times 2\delta')$ located at point $Q(x_s, y_s, 0)$ and oscillates in a simple harmonic motion over a semi-infinite body:

$$\theta(x, y, z, t) = \frac{\sqrt{\pi}}{8}\sqrt{F_o} \cdot f \int_{\Delta t=0}^{\Delta t=t} \{F(z) \cdot F(x) \cdot F(y)\} \times \frac{|\cos 2\pi(t - \Delta t)|}{\sqrt{\Delta t}} d(\Delta t) \quad [3]$$

where,

$$F(z) = \exp\left(-\frac{z^2}{2\Delta t \cdot F_o}\right), \quad F(x) = erf(A_x) + erf(B_x),$$

$$F(y) = erf(C_y) + erf(D_y)$$

$$A_x = \frac{x + A\sin(2\pi t) + A\sin(2\pi[t - \Delta t]) + \delta}{2\sqrt{F_o \Delta t}},$$

$$B_x = \frac{-x + A\sin(2\pi t) - A\sin(2\pi[t - \Delta t]) + \delta}{2\sqrt{F_o \Delta t}}$$

$$C_y = \frac{\delta + y}{2\sqrt{F_o \Delta t}}, \; D_y = \frac{\delta - y}{2\sqrt{F_o \Delta t}}$$

In Eq. [3] the symbols denote: F_o is the Fourier module and is given by $F_o = \frac{\alpha \cdot t_o}{L^2}$, where α is the thermal diffusivity, t_o the total time, L the asperity size, and δ, $F_\circ$, x, y, z, t are dimensionless. Specifically, $x = \frac{x'}{L}$, $y = \frac{y'}{L}$, $z = \frac{z'}{L}$, where x', y', z' are the Cartesian coordinates, while $t = \frac{t'}{t_o}$, with t' representing real time, $A = \frac{a}{L}$, where a is the slip amplitude (amplitude of oscillation) and $\delta = \frac{\delta'}{L}$.

Equation [3] is solved numerically using the Newton-Rahpson procedure. Inputs to the model are F_o, A, δ, f, which are constants that depend upon the material condition and the fatigue parameters.

The real temperature profile inside the specimen that undergoes fretting fatigue $T(x, y, z, t)$ is related to $\theta(x, y, z, t)$ as follows:

$$T(x, y, z, t) = \frac{\theta(x, y, z, t)}{k}[4L(\mu\sigma_f)(af)] \quad [4]$$

where k is the thermal conductivity, μ the coefficient of friction, σ_f the flow stress of the material at the surface, and f is the frequency of oscillation.

MODEL PREDICTIONS OF THE TEMPERATURE PROFILES

Model predictions of the temperature profile are presented in this section. Using Eqs. [3] and [4] the three-dimensional stress field in the heat flow channel is obtained for the following conditions:

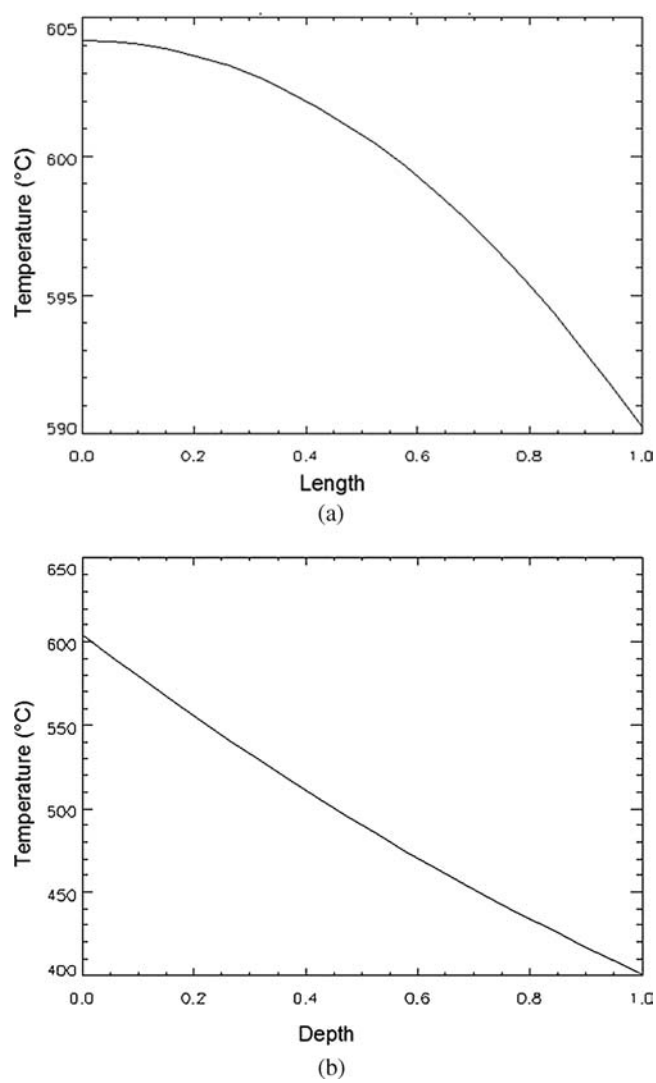

Fig. 3—Temperature versus (a) longitudinal (length: x/L), and (b) thickness (depth: z/L) directions.

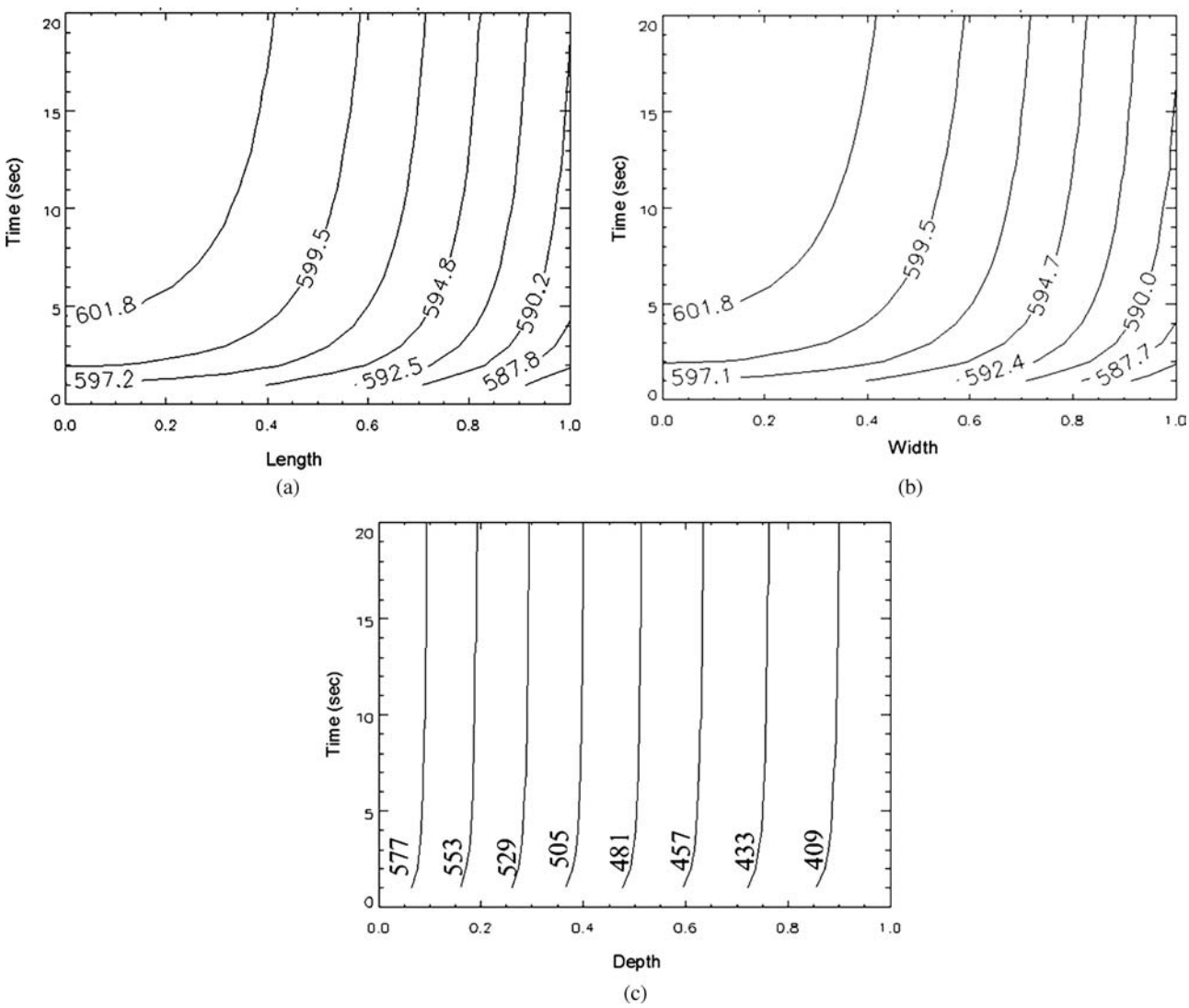

Fig. 4—Iso-temperature plots of time versus the material's (a) longitudinal (x/L), (b) transverse (y/L), and (c) thickness (z/L) directions, showing the predicted steady state temperatures.

- Motion variables: $a = 50\ \mu$m and $f = 20$ Hz
- Asperity size: L $= 10\ \mu$m
  $\delta = 5(\delta' = 5\text{L})$
- Coefficient of friction: $\mu = 0.6$

The material parameters, such as thermal conductivity k, thermal diffusivity α, and flow stress σ_f, correspond to a Ti-6Al-4V alloy and they were taken as 4.1868 W/(m·^{o}C), 1.8×10^{-6} m^2/s, and 900 MPa, respectively. Notice that some of these parameters may, more or less, vary with the particular alloy microstructure; however, we believe that they are general enough to at least obtain the general trends of the temperature profile.

The results revealed that at the beginning of the process the temperature increases quite rapidly, and it essentially reaches a constant value after approximately 1000 cycles. After this point, it is observed that the temperature variation with time is minimal. In Figs. 3a and 3b the temperature is plotted against the longitudinal (x) and depth (z) coordinates, respectively, normalized with respect to L. For both graphs $y = 0$, while in Fig. 3a $z = 0$, and in Fig. 3b $x = 0$. At first, it can be observed that the temperature reaches a high of about 600°C at the origin (near the fretting pad), confirming previous studies (Alyabev, et al. *(13)*), and it decreases at quite different rates along the x and z directions.

In particular, it is seen that the temperature decay is much faster in the z-direction in comparison to the x-direction. This observation can be attributed to the fact that there are a number of heat sources that contribute to the rise of the surface temperature ($z = 0$). On the other hand, in the z direction the heat is dissipated quite fast because the bulk of the material, which can be considered as a semi-infinite body, is and remains at a much lower, essentially room temperature.

Iso-temperature plots of time versus the material coordinates x, y, and z are presented in Figs. 4a to 4c, respectively. For any of the material coordinates the iso-temperature curves show an asymptotic behavior, which implies that a maximum value of temperature exists that a particular point inside the material can reach. Someone may argue that the maximum timescale on the graph is relatively low; however, as mentioned earlier in the

Downloaded By: [Matikas, T. E.] At: 22:02 3 March 2009

Downloaded By: [Matikas, T. E.] At: 22:02 3 March 2009

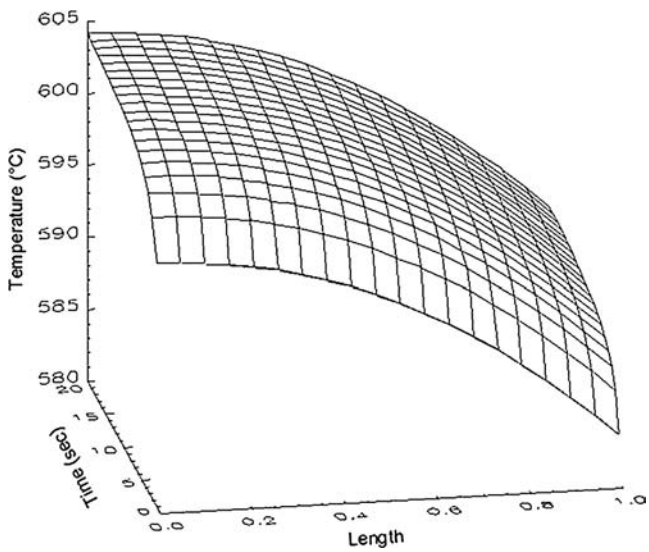

Fig. 5—Three-dimensional plot of temperature, time, and length (x/L), showing the predicted maximum temperature on the material's surface of about 600°C, which would be reached near the fretting pad after approximately 20 s of fretting fatigue testing.

article, for the temperature profiles the highest timescales are close to the steady-state ones. In addition, comparison between the graphs in Figs. 4a and 4b shows that the temperature profiles in the x and y directions are similar. Nevertheless, some very small, minor differences in temperature start to be present at higher values of length and width, with the temperature being higher in the former. This is an indication that larger differences may arise at larger distances from the origin, with the temperature in the length direction being higher because the contact body motion is along this direction. Also, a three-dimensional plot between temperature-time-length (i.e., x-coordinate) is presented in Fig. 5. This figure summarizes some of the results presented above and more clearly reveals the variation of temperature with both time and the longitudinal coordinate.

The temperature variation at the origin as a function of the frequency of oscillation is shown in Fig. 6. As the model predicts, a rise in temperature occurs with the increase in frequency of

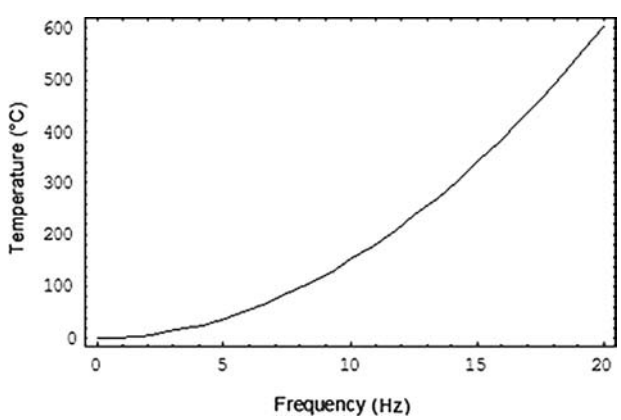

Fig. 6—Variation of temperature near the fretting pad as a function of frequency of cyclic loading.

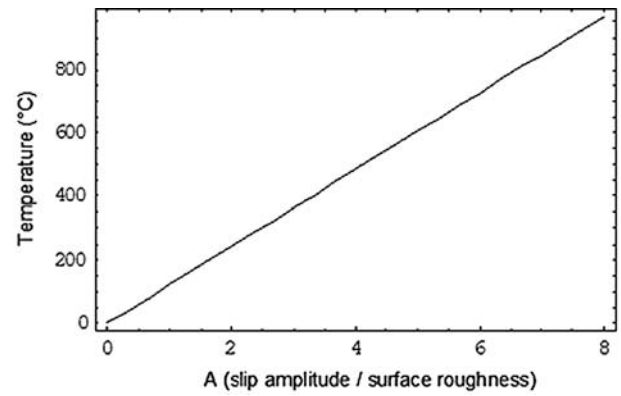

Fig. 7—Variation of temperature near the fretting pad as a function of slip amplitude, a, and the asperity size, L, of the specimen. For a value of a/L = 5, the temperature reaches a high of about 600°C.

cyclic loading. For a frequency of 20 Hz, the temperature reaches a high of about 600°C.

Finally, the temperature variation at the origin as a function of motion and contact characteristics is shown in Fig. 7. The temperature rises linearly with the increase of both the slip amplitude, a, and the asperity size, L, of the specimen. It can be observed that for a value of $A = \mathrm{a/L} = 5$ the temperature also reaches a high of about 600°C.

Equation [3] follows those of Carslaw and Jaeger *(30)* for moving heat sources. The integration is intended to account for the superposition of heating over time due to the periodic nature of the moving heat source. The heat is applied to a square of side L $= 10\ \mu$m oscillating with amplitude $\delta = 50\ \mu$m at a frequency of $f = 20$ Hz resulting in a nominal velocity of $\delta \times f = 1$ mm/s. The magnitude of the heat generated per unit area per unit time is the product of the shear stress and sliding velocity. While the formula for the heated square is not readily available, that for a heated circle is (Johnson *(31)*). The model Johnson *(31)* predicts that the heat applied to a square of side $\mathrm{L} = 10\ \mu$m oscillating with amplitude $\delta = 50\ \mu$m at a frequency of $f = 20$ Hz results in a temperature rise of only 1.3°C. Also, full-field, in situ measurements of fretting fatigue temperatures and accompanying calculations (Szolwinski, et al. *(32)*; Harish, et al. *(33)*) observed fretting temperature rises on the order of 1°C.

The apparent discrepancy between the above and the present theory and experimental results presented below is attributed to the fact that the geometry of the contact in the model (Johnson *(31)*) does not take into account the local variation of the sample's surface roughness, considering a fully flat contact area with no asperities. The present model is including an array of asperities. The temperature bearing area in the present model is quite small compared to the macroscopic flat area and hence the heat generation is concentrated over a smaller area, resulting in a much higher temperature rise.

EXPERIMENTAL VALIDATION

The theoretical predictions have been validated by fretting fatigue experiments. Both fatigue specimens and fretting pads were made of Ti-6Al-4V alloy. The specimens and pads tested in this study originated from plate stock. After forging, the Ti-6Al-4V

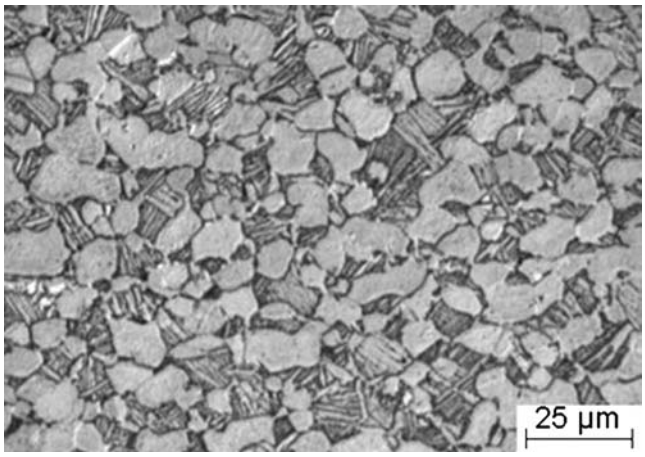

Fig. 8—Ti-6Al-4V duplex microstructure used in this study.

Downloaded By: [Matikas, T. E.] At: 22:02 3 March 2009

plate was solution heat-treated at 935°C for one hour; air fan cooled, vacuum annealed at 705°C in vacuum for two hours, then slow cooled. After processing, the plate had a duplex microstructure (Fig. 8) that consists of about 50% of equiaxed primary alpha phase and 50% of fine lamellar transformed alpha phase. This microstructure provided an ideal combination for crack initiation and crack propagation resistance together with a good tensile ductility. The slight directionality in the long axis of the plate well simulates an actual Ti-6Al-4V fan blade microstructure.

The tests were conducted using a servo-hydraulic uniaxial frame at an ambient room temperature. The experimental configuration is shown in Fig. 9. Normal fretting loads were applied to the specimens using two spring-loaded bolts. An alternating torque was applied to the end of each of the two spring-loaded bolts until the load cell located at the rear of the fretting fixture pads indicated an applied load of 1334 Newton. Longitudinal springs provided the support between the fixture plates and the load frame bracket. The surfaces of the specimens and pads tested were kept in the same as-received condition. The surface average roughness of specimens and pads was 0.19 μm. The fatigue limit for pure fatigue was 700 MPa. Fretting, however, caused a reduction of fatigue life. For example, at the 690 MPa stress level, the fretting fatigue life was only about 31,570 cycles. The fretting fatigue limit was around 200 MPa, which is about 30% of the pure fatigue limit stress. The significant reduction in fatigue life occurred at the lower stress levels, below 400 MPa.

After mechanical testing, the samples were examined using scanning electron microscopy. The surface topography clearly shows the fretting damage. The validation of the model on temperature predictions was enabled by examining the concentration of different elements in the fretting zone of a fretting-fatigued specimen using electron dispersion spectroscopy.

Figure 10a is an SEM micrograph showing the surface topography of the specimen, where the stick, the fretting, and the non-contact zones are clearly delineated. Figure 10b is an electron dispersion spectroscopy (EDS) map of the middle part of the fretting region showed in Fig. 10a, shown in concentration

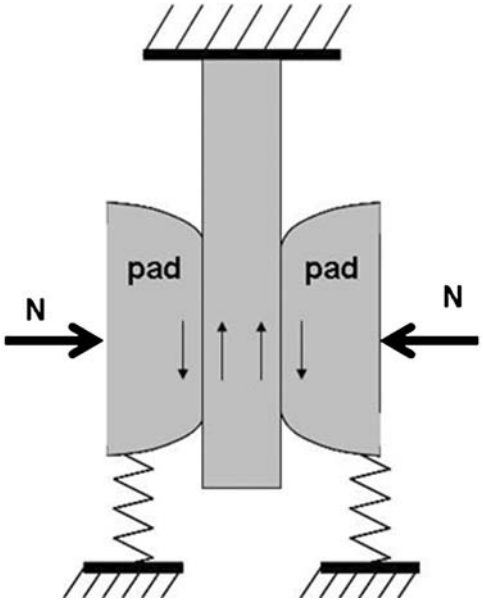

Fig. 9—Experimental configuration of the fretting fatigue setup.

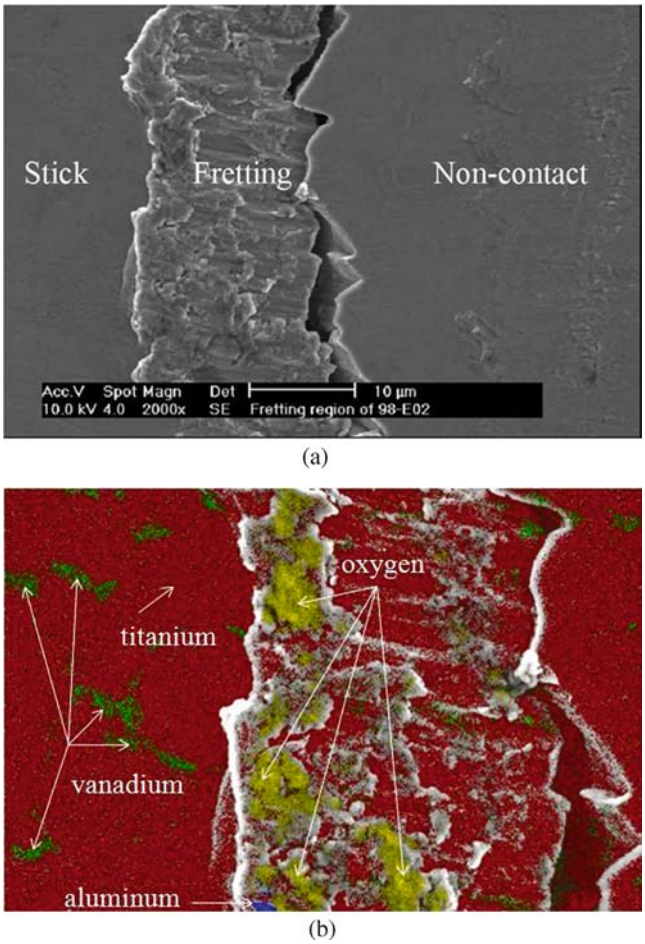

Fig. 10—Scanning electron microscopy images of a Ti-6Al-4V fretting-fatigued specimen showing: (a) the surface topography and (b) the chemical composition profile, where with arrows are shown the different elements (titanium, aluminum, vanadium, and oxygen).

of different elements (titanium in dark red, aluminum in blue, vanadium in dark green, and oxygen in light green) present on the surface of the specimen. The presence of increased oxygen concentration in the EDS map can be attributed to oxygen diffusion from the atmosphere, assisted by elevated temperatures reached during the fretting fatigue process. This observation further supports the model that predicts a significant temperature increase in the fretted region of about 600°C. It is well known that the oxygen increase during fretting fatigue depends upon the temperature and the test duration, and oxides may be formed on the surface of the specimen. Earlier work (Waterhouse *(34)*; Blanchard, et al. *(35)*; Fayeulle, et al. *(36)*) on fretting fatigue of titanium alloys (however, with a higher slip length than the one of this study) also showed an increased oxygen content and formation of TiO and TiO_2 oxides. The oxide formation was attributed to the high temperatures and interfacial stresses between the specimen and the pads. In our case, due to the small slip length, only an increase of the oxygen was observed, an increase that is not high enough for oxide formation.

CONCLUSIONS

The temperature profile during fretting fatigue for a Ti-6Al-4V alloy was determined in this work using a three-dimensional heat flow channel model. The predictions revealed a significant temperature rise of about 600°C at the heat source origin, which decays slowly in the specimen's longitudinal and transverse directions, but it decreases very rapidly in the thickness direction. The results also revealed that an essentially constant high temperature is reached after approximately 1000 fatigue cycles, causing oxidation of the contact surface. The oxygen concentration in a fretting-fatigued specimen was determined. Increased oxygen detected at the fretting zone indicates that high temperatures, in the order of those predicted by the model, had been developed during the fretting fatigue process.

REFERENCES

(1) Hoeppner, D. W. and Goss, G. L. (1974), "A Fretting-Fatigue Damage Threshold Concept," *Wear*, **27**, pp 61-70.

(2) Wharton, M. H. and Waterhouse, R. B. (1980), "Environmental Effects in the Fretting Fatigue of Ti-6Al-4V," *Wear*, **62**, pp 287-297.

(3) Lutynski, C., Simansky, G., and McEvily, A. J. (1982), "Fretting Fatigue of Ti-6Al-4V Alloy," Materials Evaluation under Fretting Conditions: ASTM STP 780, American Society for Testing and Materials, pp 150-164.

(4) Nicolaou, P. D., Shell, E. B., and Matikas, T. E. (1999), "Microstructural and Surface Characterization of Ti-6Al-4V Alloys after Fretting Fatigue," *Materials Science and Engineering A*, **269**, 1-2, pp 98-103.

(5) Nakazawa, K., Sumita, M., and Maruyama, N. (1992), "Effect of Contact Pressure on Fretting Fatigue of High Strength Steel and Titanium Alloy," In *Standardization of Fretting Fatigue Test Methods and Equipment*, ASTM STP 1159, M. Helmi Attia and R. B. Waterhouse, Eds., American Society for Testing and Materials, pp 115-125.

(6) Antoniou, R. A. and Radtke, T. C. (1997), "Mechanisms of Fretting-Fatigue of Titanium Alloys," *Materials Science and Engineering*, **A237**, pp 229-240.

(7) Asai, K. (2006), "Fretting Fatigue Strength under High Local Contact Pressure and its Fracture Mechanics Analysis," *Zairyo/Journal of the Society of Materials Science*, Japan **55**(12), pp 1102-1109.

(8) Lee, H., Mall, S., Sanders, J. H., Sharma, S. K., and Magaziner, R. S. (2007), "Characterization of Fretting Wear Behavior of Cu-Al Coating on Ti-6Al-4V Substrate," *Tribology International*, **40**(8), pp 1301-1310.

(9) Golden, P. J., Hutson, A., Sundaram, V., and Arps, J. H. (2007), "Effect of Surface Treatments on Fretting Fatigue of Ti-6Al-4V," *International Journal of Fatigue*, **29**(7), pp 1302-1310.

(10) Matikas, T. E. and Nicolaou, P. D. (2001), "Development of a Model for the Prediction of the Fretting Fatigue Regimes," *Journal of Materials Research*, **16**(9), pp 2716-2723.

(11) Wright, K. H. R. (1952), "Investigation of Fretting Corrosion," *Proc. Instn. Mech. Engrs.*, **1B**, pp 556.

(12) Waterhouse, R. B. (1961), "Influence of Local Temperature Increases on the Fretting Corrosion of Mild Steel," *J. Iron and Steel Inst.*, **197**, pp 301.

(13) Alyabev, A. Y., Kazimirchik, Yu. A., and Onoprienko, V. P. (1973), "Determination of Temperature in the Zone of Fretting Corrosion," *Soviet Materials Science*, **6**(3), pp 284-286.

(14) Archard, J. F. and Rowntree, R. A. (1988), "Metallurgical Phase Transformations in the Rubbing of Steels," *Proc. R. Soc. Lond. A*, **418**, pp 405-424.

(15) Vodopivec, F., Vizintin, J., and Sutari, B. (1996), "Effect of Fretting Amplitude on Microstructure of 1C-1.5Cr Steel," *Mater. Sci. Technol.*, **12**, pp 355-360.

(16) Podgornik, B., Kalin, M., Vizintin, J., and Vodopivec, F. (2001), "Microstructural Changes and Contact Temperatures during Fretting in Steel-Steel Contact," *J. Tribol.*, **123**, pp 670-675.

(17) Kalin, M. and Vizintin, J. (2001), "High Temperature Phase Transformations under Fretting Conditions," *Wear*, **249**(3-4), pp 172-181.

(18) Kalin, M. and Vizintin, J. (2001), "A Tentative Explanation for the Tribochemical Effects in Fretting Wear," *Wear*, **250**, pp 681-689.

(19) Pape, J. A. and Neu, R. W. (2001), "Fretting Fatigue Damage Accumulation in PH 13-8 Mo Stainless Steel," *Int. J. Fatigue*, **23**, Suppl. 1, pp 437-444.

(20) Pape, J. A. and Neu, R. W. (2007), "Subsurface Damage Development during Fretting Fatigue of High Strength Steel," *Tribology International*, **40**, pp 1111-1119.

(21) Sarkar, A. D. (1976), *Wear of Metals*, Pergamon Press, New York.

(22) Barber, J. R. (1969), "The Conduction of Heat from Sliding Solids," *Int. J. Heat Mass Transfer*, **13**, pp 857-869.

(23) Dow, T. A. (1980), "Thermoelastic Effects in a Thin Sliding Seal-A Review," *Wear*, **59**, pp 31-52.

(24) Beck, J. V. (1979), "Effects of Multiple Sources in the Contact Conductance Theory," *ASME J. Heat Transfer*, **101**, pp 132-136.

(25) Mimic, B. B. (1974), "Thermal Contact Conductance; Theoretical Considerations," *Int. J. Heat Mass Transfer*, **17**, pp 205-215.

(26) Bill, R. C. (1982), "Review of Factors that Influence Fretting Wear." In *Materials Evaluation under Fretting Conditions*, ASTM Special Technical Publication, **780**, Philadelphia, PA, pp 165-182.

(27) Wang, S. and Komvopoulos, K. (1995), "A Fractal Theory of the Temperature Distribution at Elastic Contacts of Fast Sliding Surfaces," *ASME J. Tribology*, **117**, pp 203-215.

(28) Yeo, T. and Barber, J. R. (1996), "Finite Element Analysis of the Stability of Static Thermoelastic Contact," *J. Thermal Stresses*, **19**, pp 169-184.

(29) Attia, M. H. and D'Silva, N. S. (1985), "Effect of Mode of Motion and Process Parameters on the Prediction of Temperature Rise in Fretting," *Wear*, **106**, pp 203-224.

(30) Carslaw H. S. and Jaeger J. C. (1959), *Conduction of Heat in Solids*, 2nd Ed., Oxford University Press, NY.

(31) Johnson K. L. (1985), *Contact Mechanics*, Cambridge University Press, UK.

(32) Szolwinski, M. P., Harish, G., Farris T. N., and Sakagami, T. (1999), "In-Situ Measurement of Near-Surface Fretting Contact Temperatures in an Aluminum Alloy," *ASME Journal of Tribology*, **121**(1), pp 11-19.

(33) Harish, G., Szolwinski, M. P., Farris, T. N., and Sakagami, T., (2000), "Evaluation of Fretting Stresses through Full-Field Temperature Measurements," ASTM STP **1367**, *Fretting Fatigue: Current Technologies and Practices*, D. W. Hoeppner, V. Chandrasekaran and C. B. Elliot, Eds., pp 423-435. ASTM, West Conshohocken, PA.

(34) Waterhouse, R. B. (1992), "Fretting Fatigue," *Int. Mater. Rev.*, **37(**2), pp 77-97.

(35) Blanchard, P., Colombie, C., Pellerin, V., Fayeulle, S., Vincent, L. (1991), "Material Effects in Fretting Wear: Application to Iron, Titanium, and Aluminum Alloys," *Metall. Trans. A*, **22**(7), pp 1535-1544.

(36) Fayeulle, S., Blanchard, P., and Vincent, L., (1993), "Fretting Behavior of Titanium Alloys," *STLE Tribol. Trans.*, **36**(2), pp 267-275.

Downloaded By: [Matikas, T. E.] At: 22:02 3 March 2009